Efficient Use of Solar Chargers with the Help of Ambient Light Sensors on Smartphones

Christian Schuss
University of Oulu
Oulu, Finland
christian.schuss@ee.oulu.fi

Tore Leikanger
University of Oulu
Oulu, Finland
tore.leikanger@student.oulu.fi

Bernd Eichberger
Graz University of Technology
Graz, Austria
bernd.eichberger@tugraz.at

Timo Rahkonen
University of Oulu
Oulu, Finland
timo.rahkonen@ee.oulu.fi

***Abstract*—This paper discusses the possibilities to measure the amount of light with the help of portable devices such as mobile phones and tablets. Focus is directed to the accuracy of the ambient light sensor on smartphones in order to obtain the illuminance indoors and the solar radiation level outdoors. In general, information on the ambient conditions is vital to improve the performance of solar chargers. For example, if users are able to allocate beneficial locations to deploy solar chargers inside buildings, up to 100 times more energy can be gathered during the same periodic time. Similarly, under outdoor environmental conditions, solar modules can be aligned better towards the sun to increase the possible amount of output power. We analyse the accuracy of ambient light sensors which are available in today's low-cost and upper-class smartphones. Additionally, we present calibration strategies for ambient light sensors in order to minimise the error between conventional measurement equipment and mobile phones.**

I. Introduction

Over the past number of years, mobile phones have increased significantly in terms of functionalities and possibilities [1]. Multi-core processors, fast 4G LTE (long-term Evolution) data transmission, high definition (HD) video recording and many other features have resulted into a high energy demand of today's smartphones [2], [3], [4]. In the near future, this progress is expected to continue which means the battery remains the bottleneck of portable devices. However, small gadgets such as battery packs and solar chargers are capable of overcoming low battery power until the phone can be connected for a longer period of time to get a full recharge [1].

We have discussed the opportunities to charge portable devices with solar chargers in our previous publications [5], [6], [7] and recently, we presented design specifications and guidelines for these types of chargers with the aim to satisfy user demands [8]. Photovoltaics are a type of solar technology which convert sunlight directly into electricity. Fig. 1 presents the principal system structure of solar chargers. Here, more than one photovoltaic (PV) module can be connected to the solar charger at the same time to shorten recharge times [1]. The solar charger contains a battery so that connections with smartphones are only required during the actual charging procedure of mobile phones [8], [9].

Beside the necessity of an efficient hardware topology and suitable sizes of photovoltaics [8], users play a key role in the entire system chain, which is illustrated in Fig. 1. Users have a strong impact on the amount of power which can be obtained

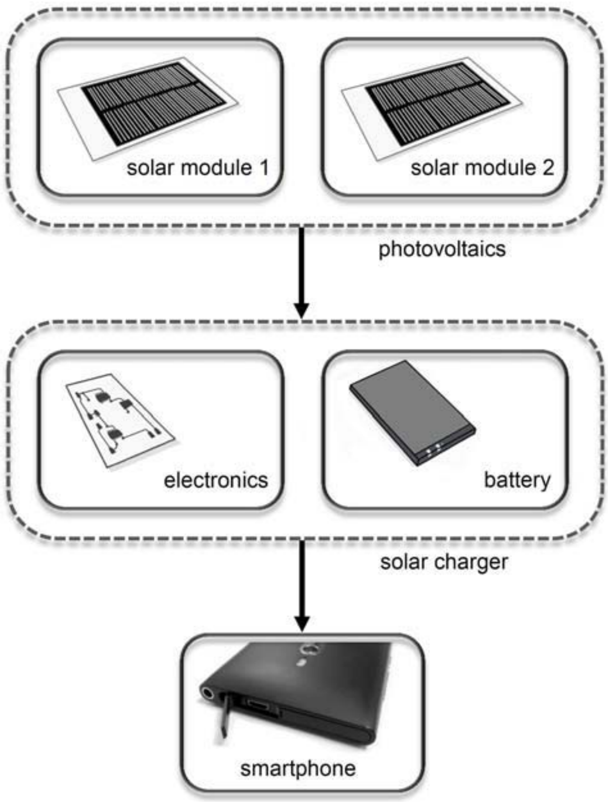

Fig. 1. Principal system structure of solar chargers

from PV modules. Solar chargers should work under indoor as well as outdoor environmental conditions. Fig. 2 illustrates a typical example for ambient conditions indoors; a library in which users sometimes do not have access to electricity from electrical sockets within reading and study areas. In such an environment, it is crucial for users to identify the most suitable location to deploy solar chargers.

Here, ambient light sensors on smartphones can be used to support users to sense their surroundings. As a result, users are able to identify the potential for solar energy production if the solar charger is either placed on the table in front of them or, for example on the bookshelf behind them. Similarly, under outdoor environmental conditions, the PV module can be aligned better towards the sun in a way that the output power from the module increases.

ISSN 2305-7254

Fig. 2. Reading and studying in an indoor environment (e.g. a library)

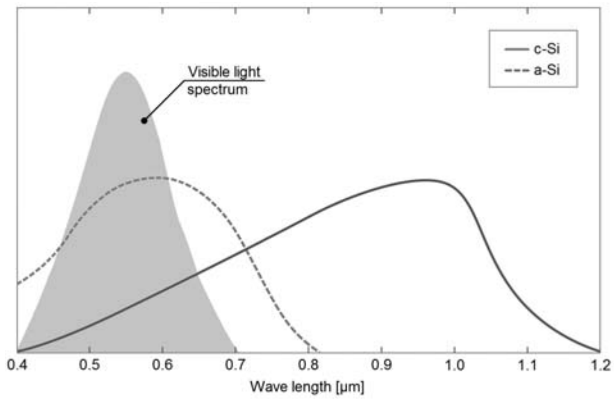

Fig. 3. Spectrum of photovoltaics and visible light spectrum

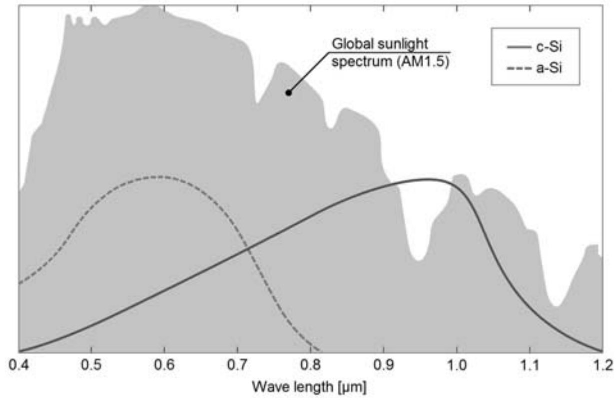

Fig. 4. Spectrum of photovoltaics and global sunlight spectrum

II. Indoor and Outdoor Environmental Conditions

In [8], we defined the output power of photovoltaics (P_{PV} [W]). This function slightly changes for indoor environmental conditions, as follows:

$$P_{PV,indoors} = f(E_V, T_c, V_{oc}, I_{sc}, A_{PV}, m_{PV}, \alpha_{PV}, d) \quad (1)$$

where E_V [lux] is the illuminance for the amount of light on surfaces, T_c [K] is the PV cell temperature, V_{oc} [V] is the open-circuit voltage, I_{sc} [A] is the short-circuit current, A_{PV} [m^2] is the size of the PV module, m_{PV} is the material of the PV module, α_{PV} [°] is the orientation of the PV module towards the light source, and d [m] is the distance of the PV module from the light source. The output power of photovoltaics outdoors can be obtained as follows:

$$P_{PV,outdoors} = f(\lambda, T_c, V_{oc}, I_{sc}, A_{PV}, m_{PV}, \alpha_{PV}) \quad (2)$$

where λ [W/m^2] is the solar radiation level. It is worth noting that E_V and λ are measured in two different physical units and therefore, there is no simple calculation between the two units. However, a conversion factor (k) can be used as an estimation allowing a basic comparison between indoor and outdoor environmental conditions, calculated as follows:

$$E_V = k \times \lambda \quad (3)$$

Suitable values for k lie in the range between 0.0015 (k_{low}) and 0.0085 (k_{high}). k as well as k_{low} and k_{high} depend, for example, on the material of the PV module (m_{PV}), the orientation of the PV module towards the light source (α_{PV}) and the spectrum of the light source. Fig. 3 illustrates the spectrum of photovoltaics compared with the visible light spectrum. Commonly, indoors, light sources are designed for the visible range of the human eye. As seen in Fig. 3, PV modules made out of amorphous silicon (a-Si) are more suitable for this wavelength range than crystalline silicion (c-Si) such as monocyrstalline and polycrystalline silicon PV modules.

However, outdoors, the situation is different. Fig. 4 illustrates the spectrum of photovoltaics compared with the global sunlight spectrum and an air mass (AM) of 1.5 which represents the available solar energy at ground level. It can be seen that PV modules made out of c-Si are able to convert a much wider wavelength range into direct electric current (DC) than PV modules manufactured from a-Si. These circumstances complicate the material choice for PV modules. Fig. 5 presents an outdoor environment. Depending on user demands, weather conditions and whether more time is spend inside or outside during the day, users should be able to choose the PV module for their solar chargers.

III. Principal Behaviour of Photovoltaics

A. Output Characteristics of Photovoltaics

Photovoltaics are of interest as a power source for portable chargers due to their high power density [10]. However, one of the disadvantages of photovoltaics lies in their strong non-linear behaviour as illustrated by the I-V (Current-Voltage) curve which demonstrates the characteristic behaviour of the output power, as shown in Fig. 6 [11], [12], [13]. This illustration is important, since the slope of the I-V curve varies between different types of photovoltaics [13]. Here, only one point exists in which the maximum amount of power can be obtained, referred as the maximum power point (MPP) [11], [12], [13].

Fig. 5. Reading and studying in an outdoor environment (e.g. a park)

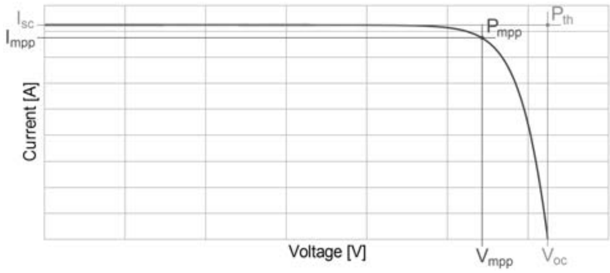

Fig. 6. I-V curve with important parameters

The fill factor (FF) is suitable for analysing the slope of the I-V curve of photovoltaics and can be calculated as follows:

$$FF = \frac{V_{mpp} \times I_{mpp}}{V_{oc} \times I_{sc}} \tag{4}$$

where V_{mpp} [V] is the voltage in the MPP, I_{mpp} [A] is the current in the MPP, P_{th} [W] is the theoretical amount of power, and P_{mpp} [W] is the power in the MPP [11], [12], [13]. As mentioned above, it is crucial to operate in the MPP. Therefore, the operating voltage (V_{op} [V]) needs to equal the voltage in the MPP (V_{mpp}). Otherwise, the amount of output power (P_{out} [W]) is less than the power in the MPP (P_{mpp}); summarised as follows:

$$\begin{cases} P_{out} = P_{mpp} & \text{if } V_{op} = V_{mpp} \\ P_{out} < P_{mpp} & \text{if } V_{op} \neq V_{mpp} \end{cases}$$

Similarly, the P-V (Power-Voltage) curve describes the performance of photovoltaics, as illustrated in Fig. 7. In the case $V_{op} \neq V_{mpp}$, the operation takes place either on the left- or right-hand side of the MPP. Here, a maximum power point tracking (MPPT) unit ensures the operation is as close to the MPP as possible [11]. Unfortunately, the position of the MPP varies with different ambient conditions and is dependent on the PV cell temperature (T_c).

Usually, under outdoor environmental conditions, the operating voltage needs to be alternated continuously. Fig. 8 presents various I-V curves on the example of a PV module (arbitrary units) at different solar radiation (λ) and temperature levels (T_c). For example, if at a solar radiation level of 600 W/m^2, the PV cell temperature drops by 10 K, the operating voltage (V_{op}) needs to be increased from $V_{mpp,1}$ to

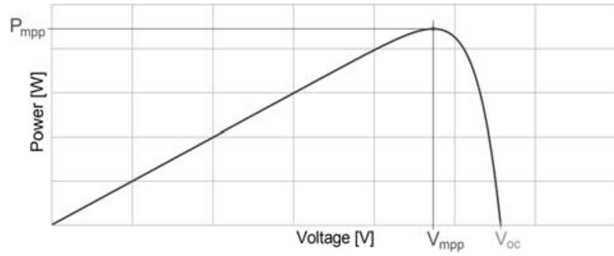

Fig. 7. P-V curve with important parameters

$V_{mpp,2}$. However, the amount of output power (P_{out}) does not only depend on a suitable MPPT algorithm and an efficient hardware topology, but also on the user of the solar charger.

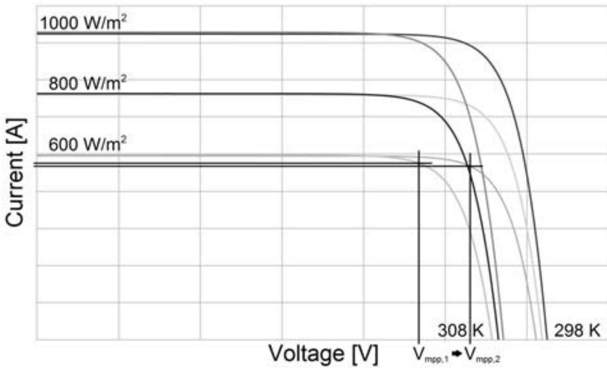

Fig. 8. Impacts of ambient conditions on the output behaviour

Beside the system efficiency of the solar charger (η [%]), a beneficial placement of PV module(s) contributes significantly to the available power on the input side of the solar charger (P_{PV}). Basically, the higher P_{PV} is, the higher P_{out} will be and, as a result, more energy will be available for charging the battery of the solar charger. This means that users have a strong influence on the charging time of their solar chargers and mobile phones. Therefore, it is vital that users are able to maximise P_{PV}, while the solar charger tries to optimise P_{out}. In this paper, we focus on the ambient light sensor (ALS) in smartphones in order to help users to maximise power from photovoltaics under given environmental conditions, either indoors or outdoors.

IV. Sensors on Smartphones

A. Types of Sensors on Smartphones

Nowadays, smartphones offer a large variety of different types of sensors for their users. We analysed mobile phones that are currently available on the market and found a connection between the amount and type of sensors with the price of the phone. At a price level of about €100 or \$125, smartphones contain on average three sensors such as an accelerometer, proximity sensor and magnetic field sensor. At a higher price level, > €200 or \$250, more sensors are included such as an additional gyro sensor and, especially, an ambient light sensor which can be used to measure the available amount of light.

However, the focus lies on the operating system (OS) of smartphones. It is important that sensor information can be accessed with the software whenever it is needed [7]. This opportunity is provided on mobile phones which run Android and Windows OSs. We include mobile phones of two market leaders who host the two different OSs in our research, Samsung and Nokia, respectively. In this paper, we investigate entry-level devices such as the Samsung Galaxy S2 Plus (GT-i9105P) and the Nokia Lumia 520, and upper-class devices such as the Samsung Galaxy S3 LTE (GT-i9305), the Samsung Galaxy Nexus (GT-i9250), and Nokia 820.

Table I summarises the types of sensors installed on Samsung smartphones while Table II presents the different sensors on Nokia smartphones. Furthermore, all smartphones possessed Bluetooth (v3.0 or v4.0), and all phones with the exception of the Nokia Lumia 520 offered the opportunity for near field communication (NFC). However, it is worth noting that the Nokia Lumia 520 was the only smartphone which offered an ALS at a price level of less than $100.

TABLE I. AVAILABLE SENSORS ON SAMSUNG SMARTPHONES

Sensor Type	S2 Plus	S3 LTE	Nexus
Ambient light sensor	x	x	x
Magnetic field sensor	x	x	x
Accelerometer	x	x	x
Proximity sensor	x	x	x
Gyro sensor	x	x	x
Pressure sensor	-	x	x

TABLE II. AVAILABLE SENSORS ON NOKIA SMARTPHONES

Sensor Type	Lumia 520	Lumia 820
Ambient light sensor	x	x
Magnetic field sensor	-	x
Accelerometer	x	x
Proximity sensor	x	x
Gyro sensor	-	x
Pressure sensor	-	-

On the smartphones in this investigation, standard applications were installed which are available free of charge to sense the amount of light intensity. Additionally, on the Android OS, hardware information can be obtained with the help of applications. Table III presents information on the parameters of the light sensors on Samsung smartphones. Here, the official range is the specified range in which the accuracy of the measurement is ensured by the manufacturer, while the maximum range represents the illuminance when the sensor becomes saturated.

TABLE III. SENSOR INFORMATION ON SAMSUNG SMARTPHONES

Information	S2 Plus	S3 LTE	Nexus
Manufacturer	Capella	Capella	Sharp
Type	CM3663	CM36651	GP2A
Function	ALS	Color-ALS	ALS
Official range	16000 lx	11796 lx	55000 lx
Maximum range	200000 lx	85745 lx	135000 lx
Consumption	0.75 mA	0.20 mA	0.75 mA

B. Comparison of Conventional Measurement Equipment

Calibrated measurement equipment was used in order to measure the illuminance (E_V) at different distances to the light source. The first measurement instrument was the Voltcraft BL-10L which was helpful in measuring and optimising the light intensity, for example, in office buildings. The maximum range is limited to 40,000 lx. Fig. 9 shows the basic luxmeter from Voltcraft. It can be seen that the sensor is directly connected to the instrument. Similarly, the ALS on smartphones is located on top of the display, either on the left- or right hand side of the speaker.

Fig. 9. Voltcraft BL-10L luxmeter

The other measurement instrument was a Vernier light sensor (LS-BTA), shown in Fig.10, which can be used either together with the Vernier SensorDAQ (data acquisition module) or the Texas Instruments (TI) Nspire CX CAS graphing calculator with a TI-Nspire lab cradle. Depending on the used equipment, the sensor information is obtained either at 13 bit-resolution (with the SensorDAQ) or at 12 bit-resolution (with the TI-Nspire) up to 150,000 lx. The sensor itself is a Hamamatsu S1133 photodiode which provides a voltage that is proportional to the light intensity.

Fig. 10. Vernier light sensor (LS-BTA)

Indoors, users are able to place solar chargers onto different objects in their surroundings such as chairs, tables, and bookshelves. Here, the distance (d) to the light source influences the amount of illuminance if the PV module is placed directly under the light source. Fig. 11 presents the measured light intensity with the Voltcraft BL-10L, while Fig. 12 shows measurement results of the Vernier light sensor under the same conditions. The relative error (ε_{rel}) can be calculated to evaluate the difference in measurement results between these two measurement instruments. Here, the mean value ($\bar{\varepsilon}_{rel}$) and standard deviation are obtained as follows:

Difference between Voltcraft BL-10L and Vernier LS-BTA:

$$\varepsilon_{rel} = +\,0.72 \pm 0.48\,\%$$

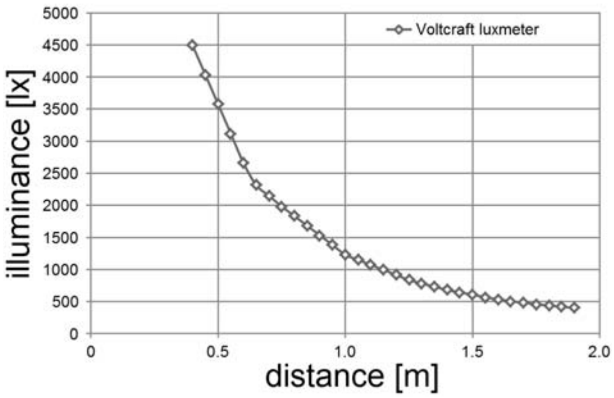

Fig. 11. Measurement results with the Voltcraft BL-10L luxmeter

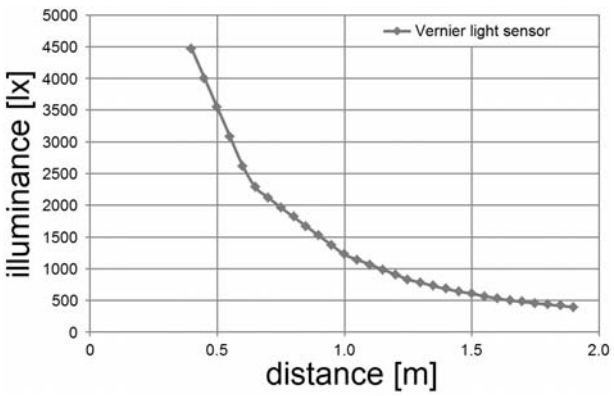

Fig. 12. Measurement results with the Vernier light sensor

C. Comparison of Ambient Light Sensors on Smartphones

Fig. 13 shows measurement results for Samsung smartphones while Fig. 14 presents measurement results for Nokia smartphones. In both cases, results are compared with the Voltcraft BL-10L. It can be seen that entry-level devices such as the Samsung Galaxy S2 Plus and the Nokia Lumia 520 detect less illuminance while upper-class devices such as the Samsung Galaxy S3 LTE and the Nokia Lumia 820 obtain more illuminance than the luxmeter from Voltcraft.

We used three Nokia Lumia 820 which contained the same hardware and OS Windows Phone 8.1. As seen in Fig. 14, even though the same mobile phone model was used, measurement results differed due to the tolerance limits of sensors. However, this relative error can be corrected by a calibration of the ambient light sensor on smartphones. Therefore, two measurements at two different distances need to be carried out by the user in order to get the required parameters for a linear regression model, summarised as follows:

$$y(x) = ax + b \quad (5)$$

$$a = \frac{y_1(x_1) - y_2(x_2)}{x_1 - x_2} \quad (6)$$

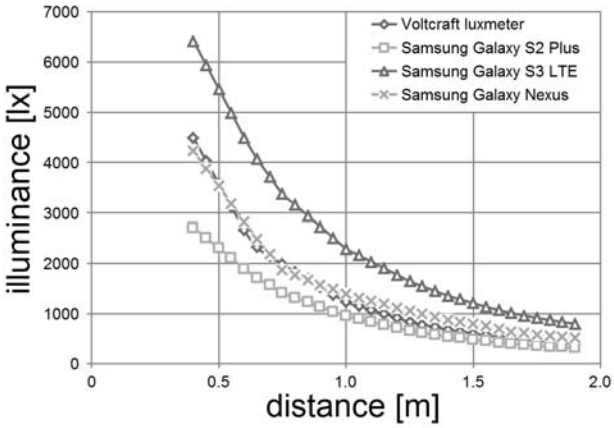

Fig. 13. Measurement results of Samsung smartphones

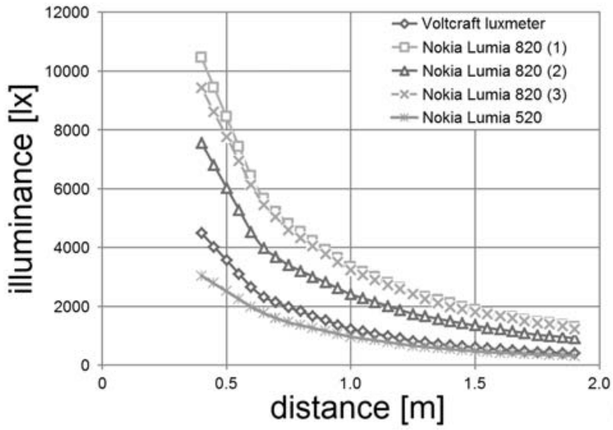

Fig. 14. Measurement results of Nokia smartphones

$$b = y_1 - ax_1 \quad \text{or} \quad b = y_2 - ax_2 \quad (7)$$

For the calibration process, the luxmeter is used as a reference on the x-axis, while the smartphone is used for the y-axis. Figures 15, 16, 17 and 18 illustrates the calibration of the Samsung Galaxy S2 Plus, Samsung Galaxy S3 LTE, Nokia Lumia 520 and one of the Nokia Lumia 820 in this investigation, respectively. It can be seen that the non-linearity is stronger on the Samsung than on Nokia smartphones. It is now possible to calculate the relative error before and after the calibration for the different smartphones.

Samsung Galaxy S2 Plus:
$\varepsilon_{rel} = -23.99 \pm 5.52\,\%$ before calibration
$\varepsilon_{rel} = +2.90 \pm 9.97\,\%$ after calibration

Samsung Galaxy S3 LTE:
$\varepsilon_{rel} = +88.10 \pm 17.39\,\%$ before calibration
$\varepsilon_{rel} = +3.00 \pm 10.76\,\%$ after calibration

Nokia Lumia 520:
$\varepsilon_{rel} = +88.10 \pm 17.39\,\%$ before calibration
$\varepsilon_{rel} = +1.72 \pm 5.75\,\%$ after calibration

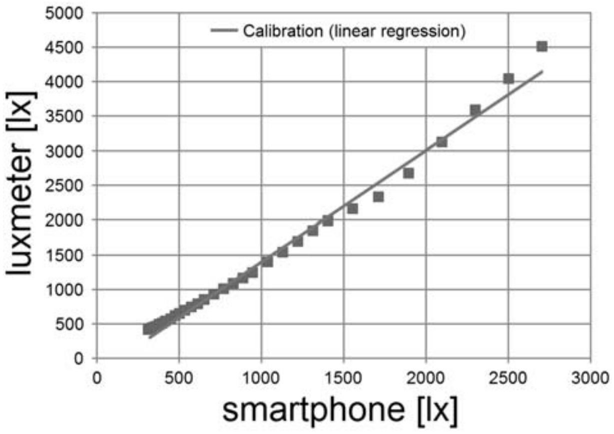

Fig. 15. Calibration of the Samsung Galaxy S2 Plus

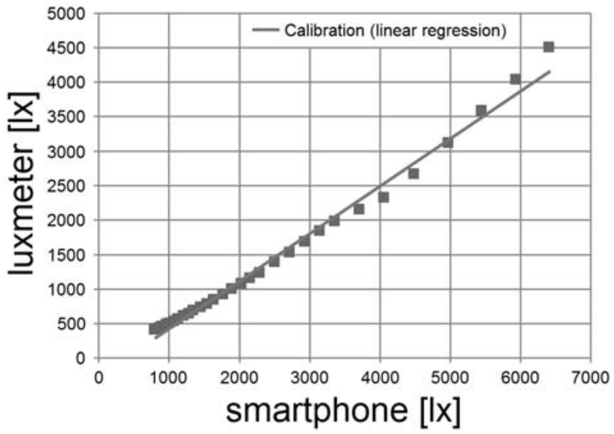

Fig. 16. Calibration of the Samsung Galaxy S3 LTE

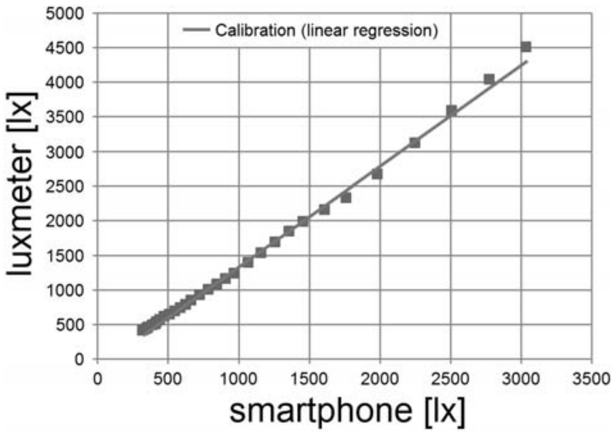

Fig. 17. Calibration of the Nokia Lumia 520

Nokia Lumia 820 (1):

$\varepsilon_{rel} = +190.91 \ \pm 34.70\,\%$ before calibration

$\varepsilon_{rel} = +0.56 \ \pm 4.19\,\%$ after calibration

However, outdoors, it is difficult to measure the solar radiation (λ) with the help of ambient light sensors on smartphones. Here, the Voltcraft PL-110SM is employed as the reference measurement instrument. Fig. 19 shows the measurement instrument on which the sensor is separated from the measurement tool while Fig. 20 presents the illuminance [lx] obtained by different smartphones compared with the measured solar radiation level [W/m^2]. In Fig. 20 the error levels are much more non-linear and, as a result, the search for a suitable regression between smartphones from different manufacturers is complicated. It is worth noting that outdoors users will be able to optimise the orientation angle towards the sun of the PV module with the help of the ALS, as illustrated in Fig. 21.

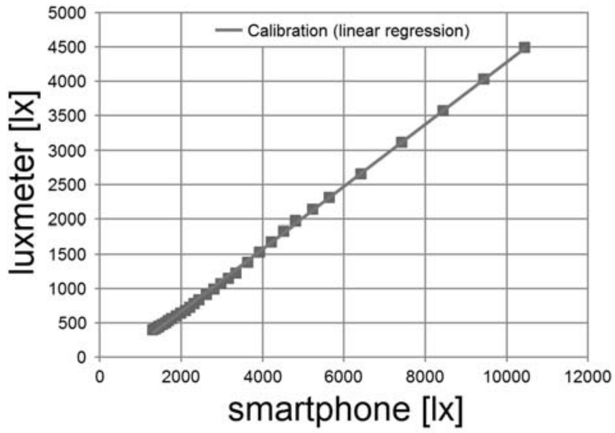

Fig. 18. Calibration of the Nokia Lumia 820 (1)

Fig. 19. Voltcraft PL-110SM solar radiation measurement instrument

V. DISCUSSION

In this paper, we focused on ambient light sensors in smartphones in order to help users in finding suitable locations for solar chargers. It is worth noting that the measured amount of light directly influences the available amount of power from photovoltaics. Our results on the accuracy of sensors are

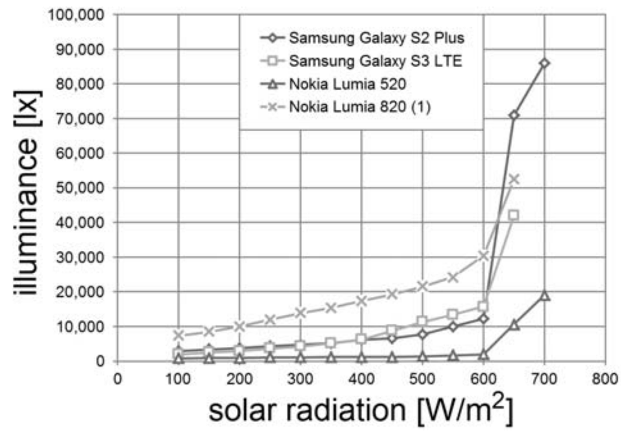

Fig. 20. Comparison of measured illuminance vs. solar radiation level

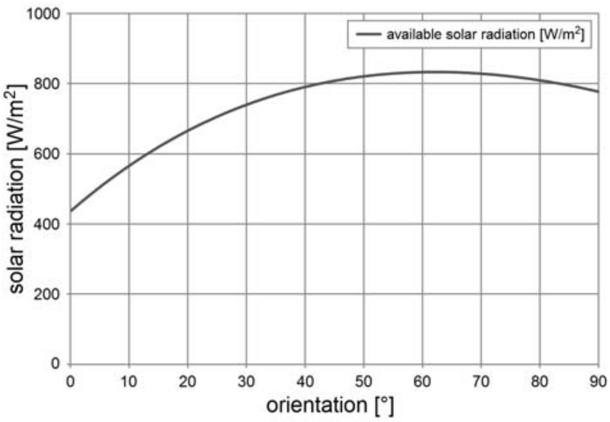

Fig. 21. Influence of different orientation angles towards the sun

also useful for other types of applications. For example, data from ambient light sensors in smartphones can be useful to evaluate the light exposure of humans on a daily basis [14]. Periodic measurements are vital in order to estimate the overall amount of light. As a result, the daily illuminance can be studied and light deficits can be recognised. Here, the accuracy of light sensors is important when data is recorded under indoor and outdoor environmental conditions. The magnitude of error depends on the type of smartphone. We even found a connection between the price level of the mobile phone and the size of the error. Variations need to be taken into account when data is recorded with different types of smartphones [14].

VI. Conclusion

Ambient light sensors of Samsung and Nokia smartphones show a surprisingly large error range in comparison to conventional measurement equipment. Even though manufacturers report in their data sheets of an accuracy of $\pm$ 15 %, measured values differed up to 200 % from each other. However, the non-linear error level makes it difficult to calibrate the ambient light sensors of smartphones. For indoor environmental conditions, we presented calibrations strategies which help to significantly reduce the relative error level. Therefore, users are able to evaluate locations which are more or less suitable for deploying solar chargers. Moreover, users are interested in the energy predictions of smartphones.

Acknowledgment

We wish to thank Infotech Oulu, the Nokia Foundation, the Tauno Tönning Foundation, and the Faculty of Information Technology and Electrical Engineering of the University of Oulu for financially supporting this research.

References

[1] D. Ferreira, A.K. Dey, and V. Kostakos, "Understanding Human-Smartphones Concerns: A Study of Battery Life", *Lecture Notes in Computer Science*, vol. 6696, 2011, pp. 19-33.

[2] D. Jia, Y. Duan, and J. Liu, "Emerging technologies to power next generation mobile phone electronic devices using solar energy", *Frontiers of Energy and Power Engineering in China*, vol. 3, issue: 3, 2009, pp. 262-288.

[3] D. Ferreira, E. Ferreira, J. Goncalves, V. Kostakos, and A.K. Dey, "Revisiting Human-Battery Interaction With An Interactive Battery Interface", *Proceedings of the 2013 ACM International Joint Conference on Pervasive and Ubiquitous Computing (UbiComp)*, 2013, pp. 563-572.

[4] C. Li, W. Jia, Q. Tao, and M. Sun, "Solar Cell Phone Charger Performance in Indoor Environment", *IEEE 37th Annual Northeast Bioengineering Conference (NEBEC)*, 2011, art. no. 5778623.

[5] C. Schuss, and T. Rahkonen, "Use of Mobile Phones as Microcontrollers for Control Applications such as Maximum Power Point Tracking (MPPT)", *Proceedings of the IEEE 16th Mediterranean Electrotechnical Conference (MELECON)*, 2012, pp. 792-795.

[6] C. Schuss, and T. Rahkonen, "Photovoltaic (PV) Energy as Recharge Source for Portable Devices such as Mobile Phones", *Proceedings of the 12th Conference of FRUCT Association*, 2012, pp. 120-128.

[7] C. Schuss, and T. Rahkonen, "Solar Energy Harvesting Strategies for Portable Devices such as Mobile Phones", *Proceedings of the 14th Conference of FRUCT Association*, 2013, pp. 132-139.

[8] C. Schuss, B. Eichberger, and T. Rahkonen, "Design Specifications and Guidelines for Efficient Solar Chargers of Mobile Phones", *11th International Multi-Conference on Systems, Signals Devices (SSD)*, 2014, pp. 1-5.

[9] S. Park, B. Koh, Y. Wang, J. Kim, Y. Kim, M. Pedram, and N. Chang, "Maximum Power Transfer Tracking in a Solar USB Charger for Smartphones", *IEEE International Symposium on Low Power Electronics and Design (ISLPED)*, 2013, pp. 88-93.

[10] V. Raghunathan, A. Kansal, J. Hsu, J. Friedman, and M. Srivastava, "Design considerations for solar energy harvesting wireless embedded systems", *4th International Symposium on Information Processing in Sensor Networks*, 2005, pp. 457-462.

[11] T. Esram, and P.L. Chapman, "Comparison of Photovoltaic Array Maximum Power Point Tracking Techniques", *IEEE Transactions on Energy Conversion*, vol. 22, issue: 2, 2007, pp. 439-449.

[12] M.A. Green, "General solar cell curve factors including the effects of ideality factor, temperature and series resistance", *Solid State Electronics*, vol. 20, issue: 3, 1977, pp. 265-266.

[13] C. Schuss, B. Eichberger, and T. Rahkonen, "Measurement and Verification of Photovoltaic (PV) Simulation Models", *Proceedings of the IEEE International Instrumentation and Measurement Technology Conference (I2MTC)*, 2013, pp. 188-193.

[14] F. Wahl, T. Kantermann, and O. Amft, "How Much Light Do You Get?: Estimating Daily Light Exposure Using Smartphones", *Proceedings of the 2014 ACM International Symposium on Wearable Computers*, 2014, pp. 43-46.